Figure S1 **Normalization procedure and filtering criteria**

(A) In order to correct for potential mixing errors, TMT data were normalized based on the assumption that the total protein amount (light and heavy labeled protein) is equal across time-points (see also supplementary methods). This procedure decreased the variance of the data and improved the coefficient of determination (R^2) of the curve fit, ultimately increasing the number of peptide evidence entries passing the filter criteria after curve fitting for the rate K, the coefficient of determination R^2, the curve maximum A and the offset B ("KRAB"-filter). (B) For half-life calculations, rates of cell doubling were determined by cell counting for all four cell culture replicates separately in order to account for even minor differences in growth behavior, for instance, due to variation in cell density before cell passage or initial seeding density.

Figure S2 **Comparison of MS1, MS2 and MS3 based methods for protein turnover rate estimation**

(A) TMT labeled pulsed SILAC lysates were fractionated into 6 fractions and measured using a MS2 and MS3 based method. Boxplots (10^{th}-90^{th} percentile) of TMT intensity ratios show that MS2 based quantification suffered from ratio compression which severely distorted subsequent curve fittings and rate estimations. (B) Correlation matrix depicts color-coded Pearson's correlation coefficients for log transformed protein rates between the present study and previously published datasets. Numbers inside cells indicate the number of proteins available for each correlation analysis.

Figure S3 **Reproducibility of peptide rate determination by pulsed SILAC-TMT labeling**

(A) Correlation matrix depicts color-coded Pearson's correlation coefficients for log transformed peptide turnover rates determined from synthesis and degradation curves for cell culture (R1-R4) and MS injection (R2 and R2') replicates. The boxplots (10^{th}-90^{th} percentile) show the coefficients of variation of peptide turnover rates across replicate MS injections, synthesis and degradation curves pairs within a sample and

cell culture replicates. For some peptides, the precision of rate determination from increasing versus decreasing curves was compromised by residual ratio compression which deteriorated correlations. (B) Ratio distortion in particular affects curves of high turnover peptides (large values for K) as suggested by the positive correlation of rates and CVs computed from synthesis and degradation curve pairs (R: Pearson's correlation coefficient). (C) CVs across technical replicates did not correlate with rates indicating that synthesis and degradation behavior of fast and slow turnover peptides can be identified with a comparably high precision. (D) Good agreement of peptide curve fits across cell culture replicates is exemplified for the fast turnover protein G2/mitotic-specific cyclin-B1 (CCNB1) and the very stable 60S ribosomal protein L32 (RPL32).

Figure S4 **Biophysical and functional determinants of cellular protein stability**

(A) The percentage of canonical protein isoforms in functional Gene Ontology (GO) and UniProt Keyword categories was highly correlated for all proteins from the database and the subset of proteins for which turnover rates were determined in this study (BP: biological process; MF: molecular function; CC: cellular compartment). Only membrane associated and extracellular proteins were underrepresented in the set of identified proteins. (B) Protein copies per cell, which were computed utilizing TMT and MS1 intensity information (see supplementary methods), showed a strong correlation with absolute quantitative data published by Nagaraj *et al.* (1) and Zeiler *et al.* (2). (C) Copies of proteins for which rates of turnover were determined spanned seven orders of magnitude. (D) Violin plots display that the 10 % most and least stable proteins (n=700) differed significantly in the proportion of hydrophobic and polar amino acids as well as in the fraction of disordered secondary structure. (E) Correlation matrix indicates Spearman rank correlation coefficients illustrating that protein features are interdependent exhibiting, for instance, a moderate negative correlation between copies per cell and the sequence length of proteins. (F) No significant difference of cellular protein half-lives was identified between the three categories of thermal

stability determined by Leuenberger *et al.* (3). Numbers display the number of proteins in the respective category. (G) Enzymes which were significantly enriched in stable proteins distinctively differed in abundance, primary and secondary structure from transcription factors which were much less stable.

Figure S5 **Impact of oxidative stress on the turnover of respiratory chain complex I proteins**

(A) HeLa cells grown in K0/R0 (light) medium were treated with 1 uM rotenone (complex I inhibitor) and 5 mM glutamate and malate (complex I specific substrates) to induce oxidative stress. After 30 min, cells were pulsed with K8/R10 (heavy) medium to enable an identification of newly synthesized proteins by the SILAC label. (B, C, D) Volcano plots illustrate that, after a 3 and 8h pulse with K8/R10 medium, the heavy-to-light ratios of peptides belonging to NADH dehydrogenase proteins exhibited an overall shift towards higher ratios upon rotenone inhibition compared to the control treatments suggesting an accelerated turnover due to increased oxidative stress. Significantly changing peptides are displayed by filled circles (two-sided t-test, n=3, S0=0.05, 5 % FDR).

Figure S6 **Analysis of proteoform resolved protein turnover**

(A) Correlation analysis of log transformed labeling rates for oxidized peptides and their non-oxidized counterparts showed no global influence of detected oxidation on turnover. The analysis included peptide pairs from all 4 replicates (11,314 in total). (B) Turnover rates of all peptides were matched to corresponding protein rates and tested for significant differences in a two-sided t-test (S0=0.048, 5 % FDR). Peptides exhibiting significantly differing rates are colored in blue. (C) N-terminal peptides rates were compared against each other and the associated protein rates in a two-sided t-test (S0=0.04, 5 % FDR). Significantly different pairs are annotated and also displayed in Fig. 6C. (D) The propeptides of prosaposin appeared to be much less stable than the mature saposins. Peptides encompassing the cleavage site of saposin B and the following propeptide showed a slower turnover comparable to saposin

A, C and D, whereas peptides comprising the cleavage site of saposin A and the successive propeptide showed a faster turnover matching that of propeptides (for saposin B no peptides were detected, dotted lines indicate peptides that span cleavage sites).

1. Nagaraj, N., Wisniewski, J. R., Geiger, T., Cox, J., Kircher, M., Kelso, J., Pääbo, S., and Mann, M. (2011) Deep proteome and transcriptome mapping of a human cancer cell line. *Molecular systems biology* 7

2. Zeiler, M., Straube, W. L., Lundberg, E., Uhlen, M., and Mann, M. A Protein Epitope Signature Tag (PrEST) Library Allows SILAC-based Absolute Quantification and Multiplexed Determination of Protein Copy Numbers in Cell Lines.

3. Leuenberger, P., Ganscha, S., Kahraman, A., Cappelletti, V., Boersema, P. J., von Mering, C., Claassen, M., and Picotti, P. (2017) Cell-wide analysis of protein thermal unfolding reveals determinants of thermostability. *Science* 355

Fig. S1

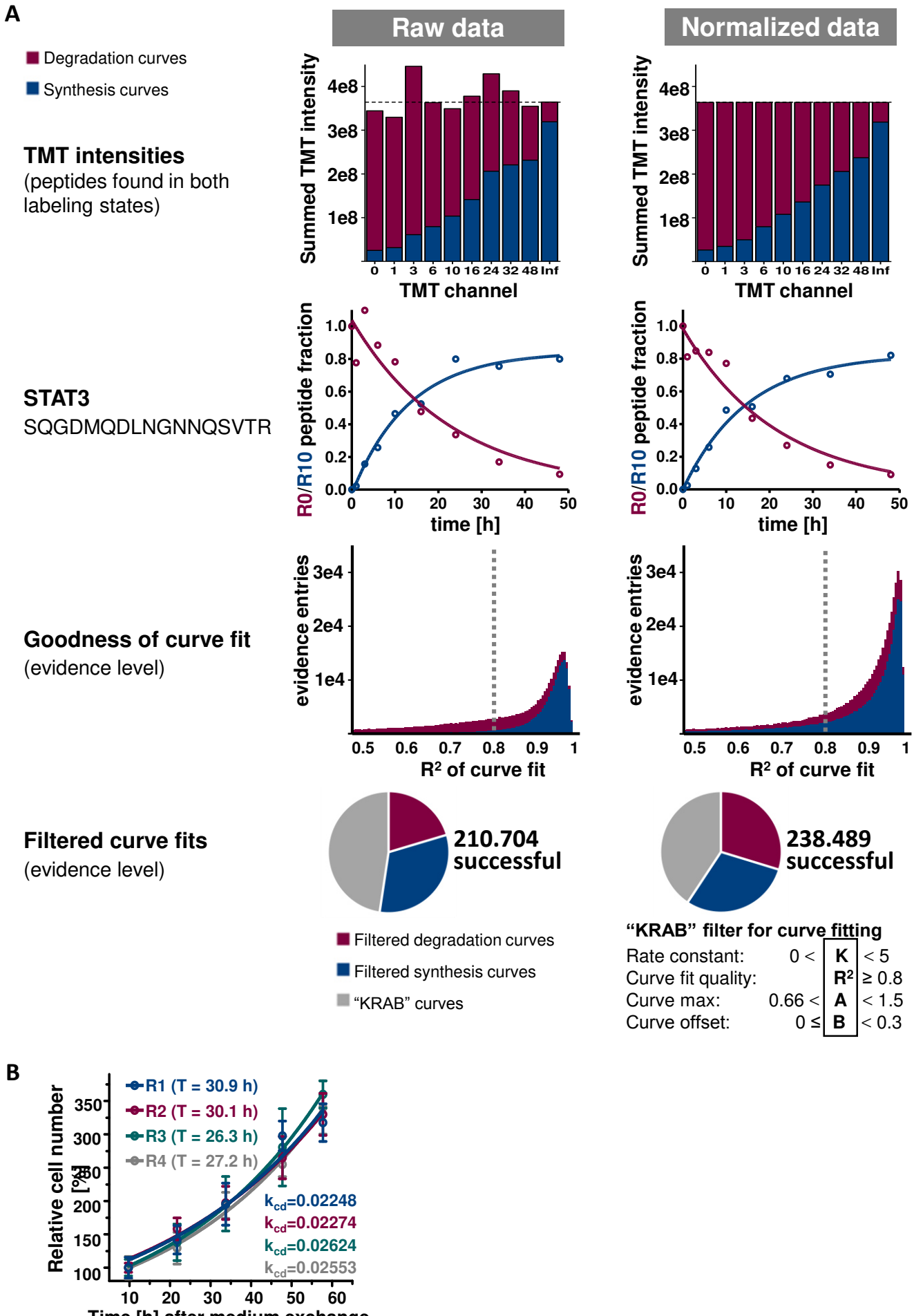
A
Raw data
Normalized data
Degradation curves
Synthesis curves
TMT intensities
(peptides found in both labeling states)
Summed TMT intensity
TMT channel
STAT3
SQGDMQDLNGNNQSVTR
R0/R10 peptide fraction
time [h]
Goodness of curve fit
(evidence level)
evidence entries
R² of curve fit
Filtered curve fits
(evidence level)
210.704 successful
238.489 successful
Filtered degradation curves
Filtered synthesis curves
"KRAB" curves
"KRAB" filter for curve fitting
Rate constant: 0 < K < 5
Curve fit quality: R² ≥ 0.8
Curve max: 0.66 < A < 1.5
Curve offset: 0 ≤ B < 0.3
B
R1 (T = 30.9 h)
R2 (T = 30.1 h)
R3 (T = 26.3 h)
R4 (T = 27.2 h)
Relative cell number [%]
Time [h] after medium exchange
kcd=0.02248
kcd=0.02274
kcd=0.02624
kcd=0.02553

Fig. S2

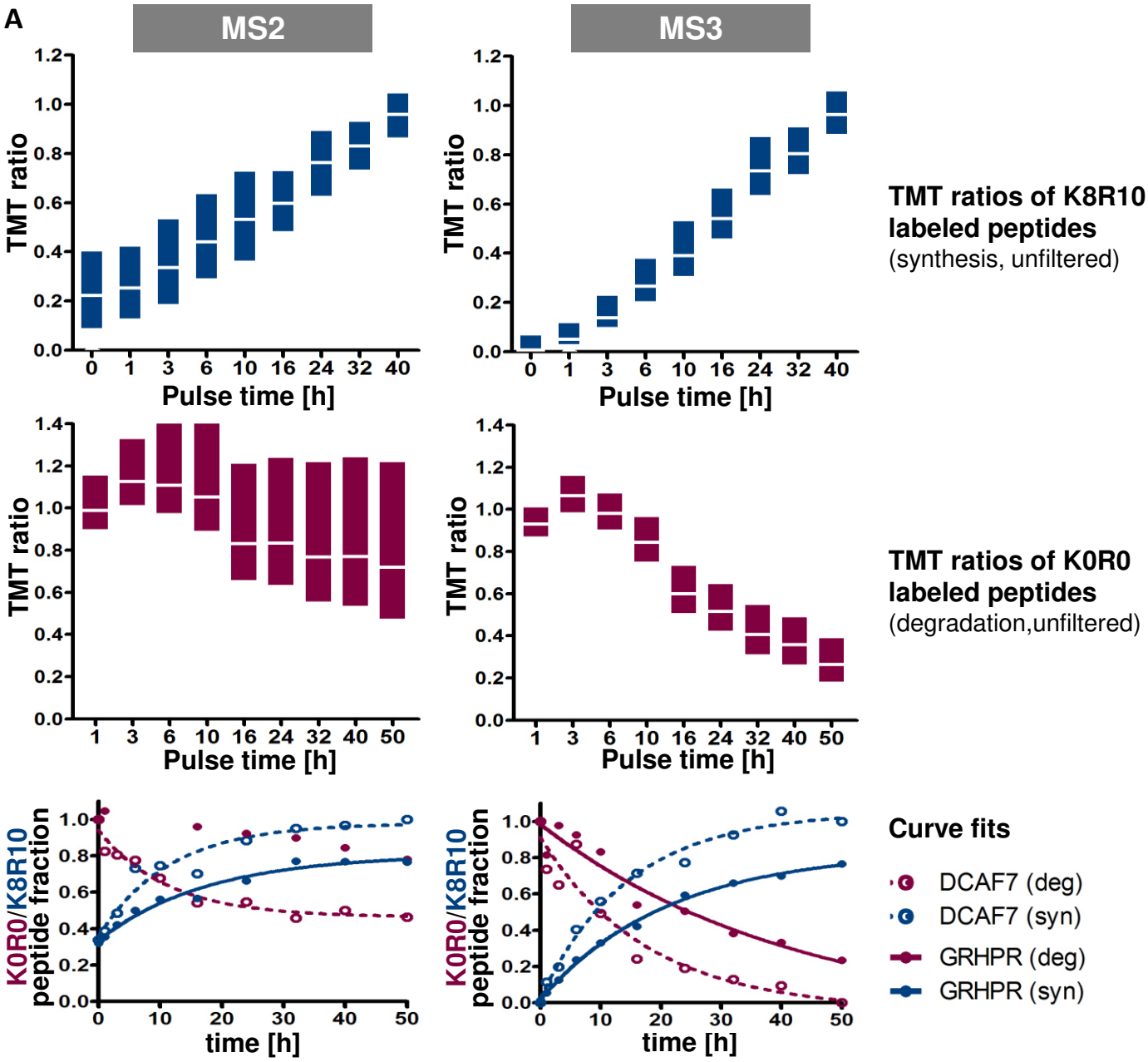
A
MS2
MS3
TMT ratio
Pulse time [h]
TMT ratios of K8R10 labeled peptides
(synthesis, unfiltered)
TMT ratios of K0R0 labeled peptides
(degradation,unfiltered)
K0R0/K8R10 peptide fraction
time [h]
Curve fits
DCAF7 (deg)
DCAF7 (syn)
GRHPR (deg)
GRHPR (syn)

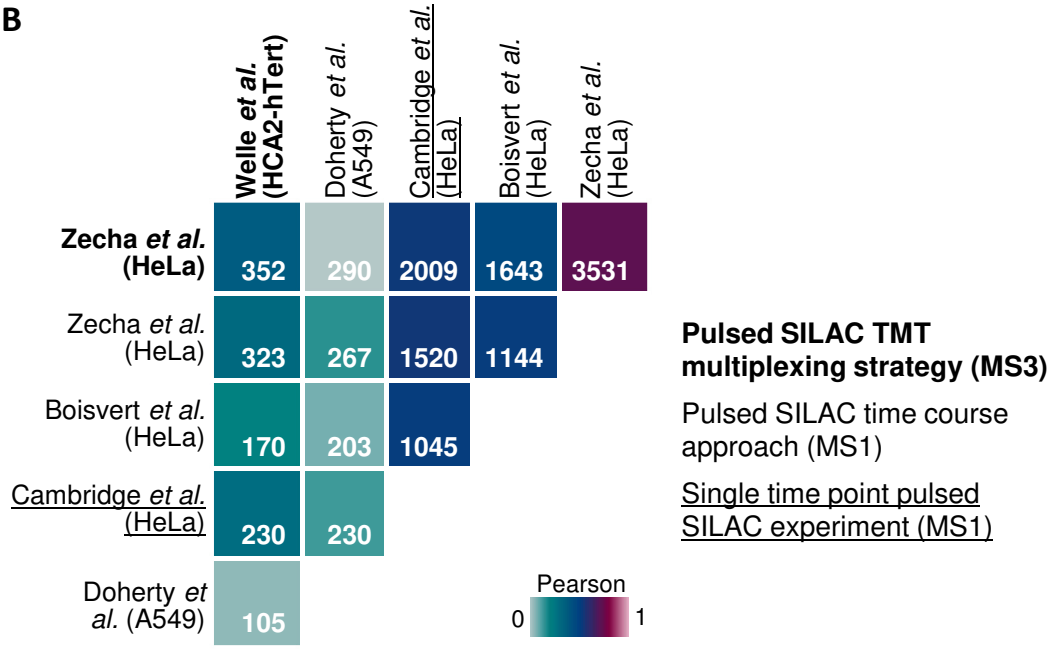
B
Welle et al. (HCA2-hTert)
Doherty et al. (A549)
Cambridge et al. (HeLa)
Boisvert et al. (HeLa)
Zecha et al. (HeLa)
Zecha et al. (HeLa)
352
290
2009
1643
3531
Zecha et al. (HeLa)
323
267
1520
1144
Boisvert et al. (HeLa)
170
203
1045
Cambridge et al. (HeLa)
230
230
Doherty et al. (A549)
105
Pearson
0
1
Pulsed SILAC TMT multiplexing strategy (MS3)
Pulsed SILAC time course approach (MS1)
Single time point pulsed SILAC experiment (MS1)

Fig. S3

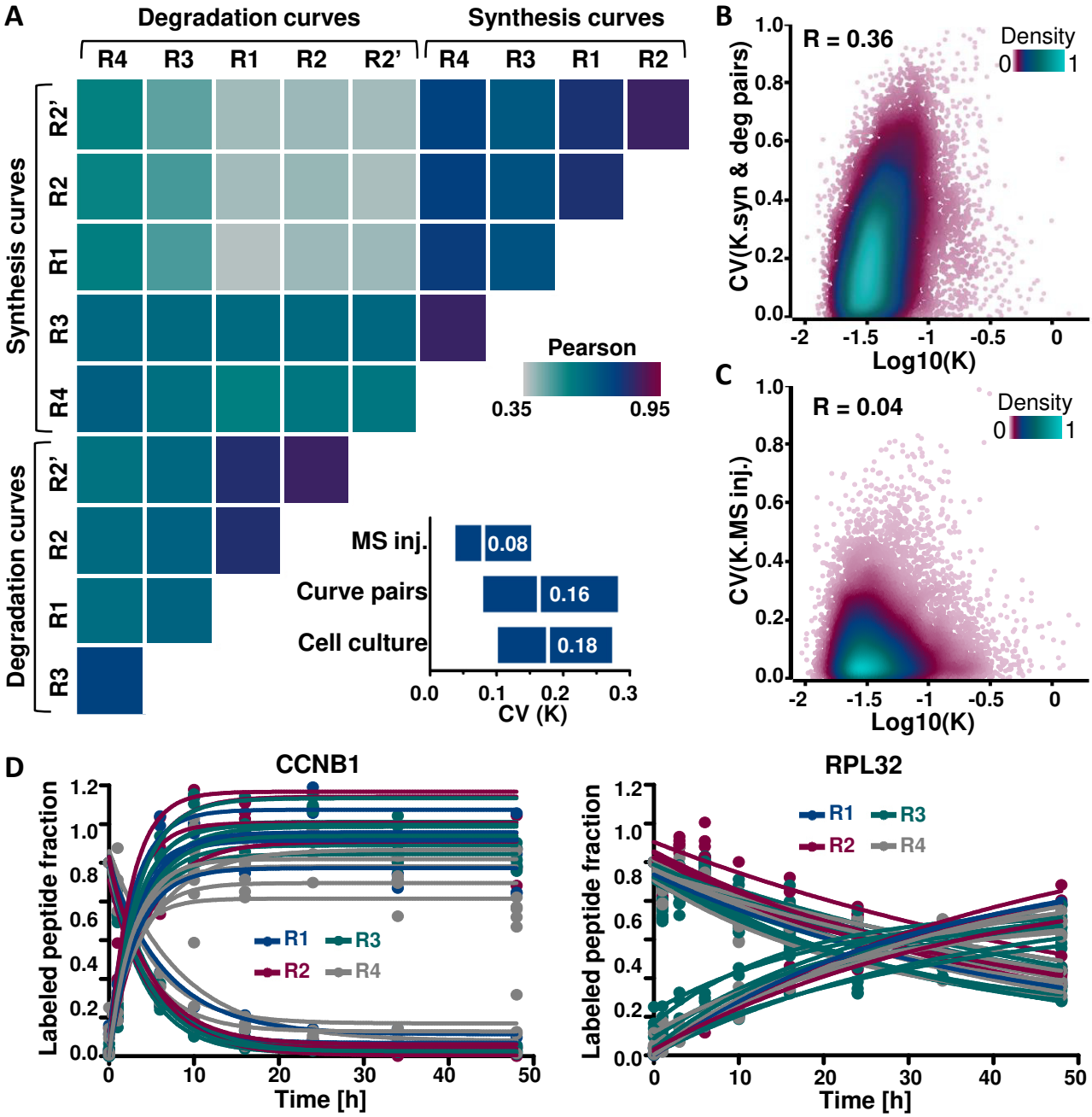
A
Degradation curves
Synthesis curves
R4 R3 R1 R2 R2'
R4 R3 R1 R2
Synthesis curves
R2' R2 R1 R3 R4
Degradation curves
R2' R2 R1 R3
Pearson
0.35 0.95
MS inj. 0.08
Curve pairs 0.16
Cell culture 0.18
0.0 0.1 0.2 0.3
CV (K)
B
R = 0.36
Density
0 1
CV(K.syn & deg pairs)
Log10(K)
C
R = 0.04
Density
0 1
CV(K.MS inj.)
Log10(K)
D
CCNB1
RPL32
Labeled peptide fraction
Time [h]
R1 R3
R2 R4

Fig. S4

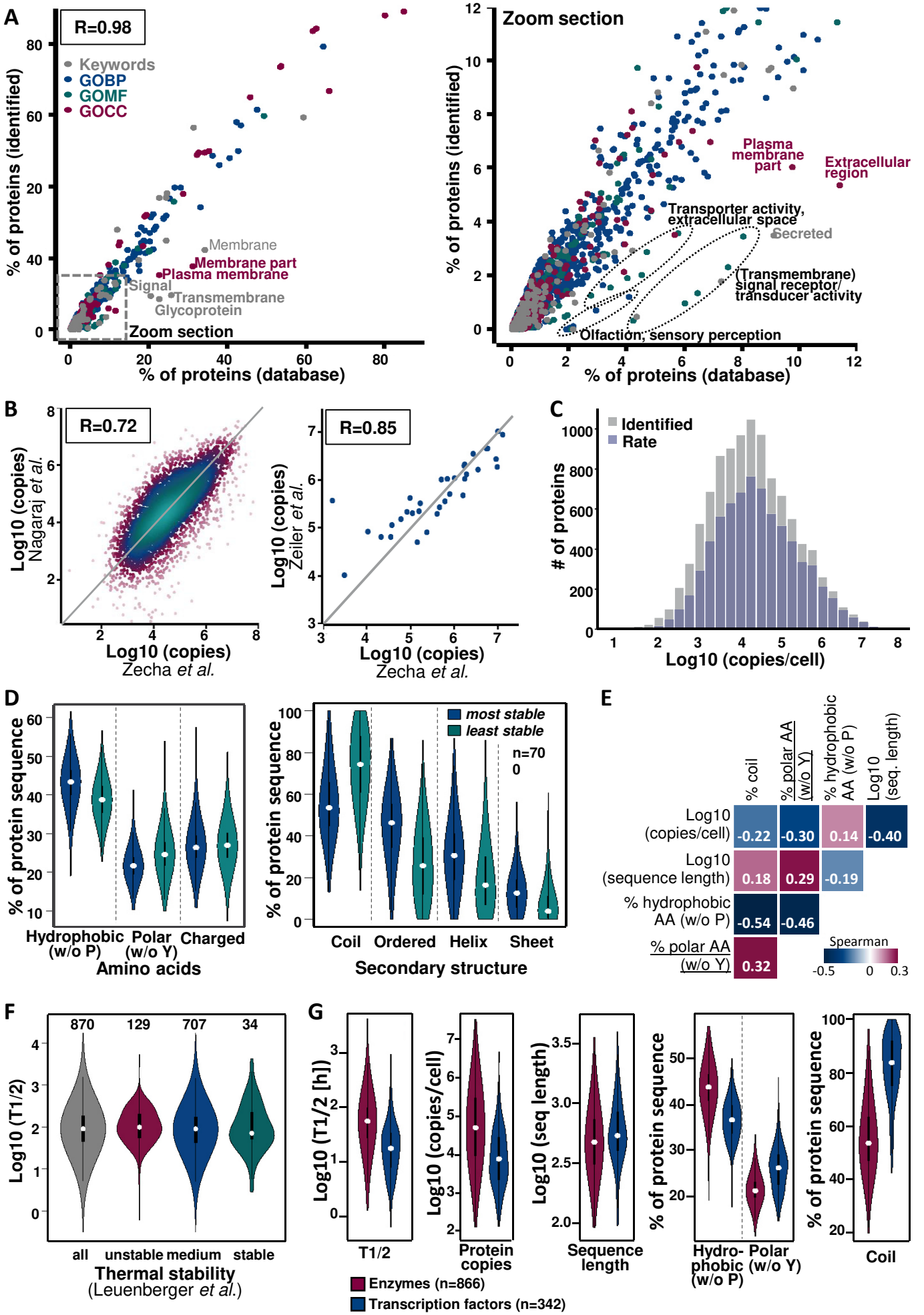
A
R=0.98
Keywords
GOBP
GOMF
GOCC
Membrane
Membrane part
Plasma membrane
Signal
Transmembrane
Glycoprotein
Zoom section
% of proteins (identified)
% of proteins (database)
Zoom section
Plasma membrane part
Extracellular region
Transporter activity, extracellular space
Secreted
(Transmembrane) signal receptor/ transducer activity
Olfaction, sensory perception
B
R=0.72
Log10 (copies) Nagaraj et al.
Log10 (copies) Zecha et al.
R=0.85
Log10 (copies) Zeiler et al.
Log10 (copies) Zecha et al.
C
Identified
Rate
# of proteins
Log10 (copies/cell)
D
% of protein sequence
Hydrophobic (w/o P)
Polar (w/o Y)
Charged
Amino acids
most stable
least stable
n=70
0
Coil
Ordered
Helix
Sheet
Secondary structure
E
% coil
% polar AA (w/o Y)
% hydrophobic AA (w/o P)
Log10 (seq. length)
Log10 (copies/cell)
Log10 (sequence length)
% hydrophobic AA (w/o P)
% polar AA (w/o Y)
-0.22
-0.30
0.14
-0.40
0.18
0.29
-0.19
-0.54
-0.46
0.32
Spearman
-0.5
0
0.3
F
870
129
707
34
Log10 (T1/2)
all
unstable
medium
stable
Thermal stability
(Leuenberger et al.)
G
Log10 (T1/2 [h])
T1/2
Log10 (copies/cell)
Protein copies
Log10 (seq length)
Sequence length
% of protein sequence
Hydro-phobic (w/o P)
Polar (w/o Y)
% of protein sequence
Coil
Enzymes (n=866)
Transcription factors (n=342)

Fig. S5

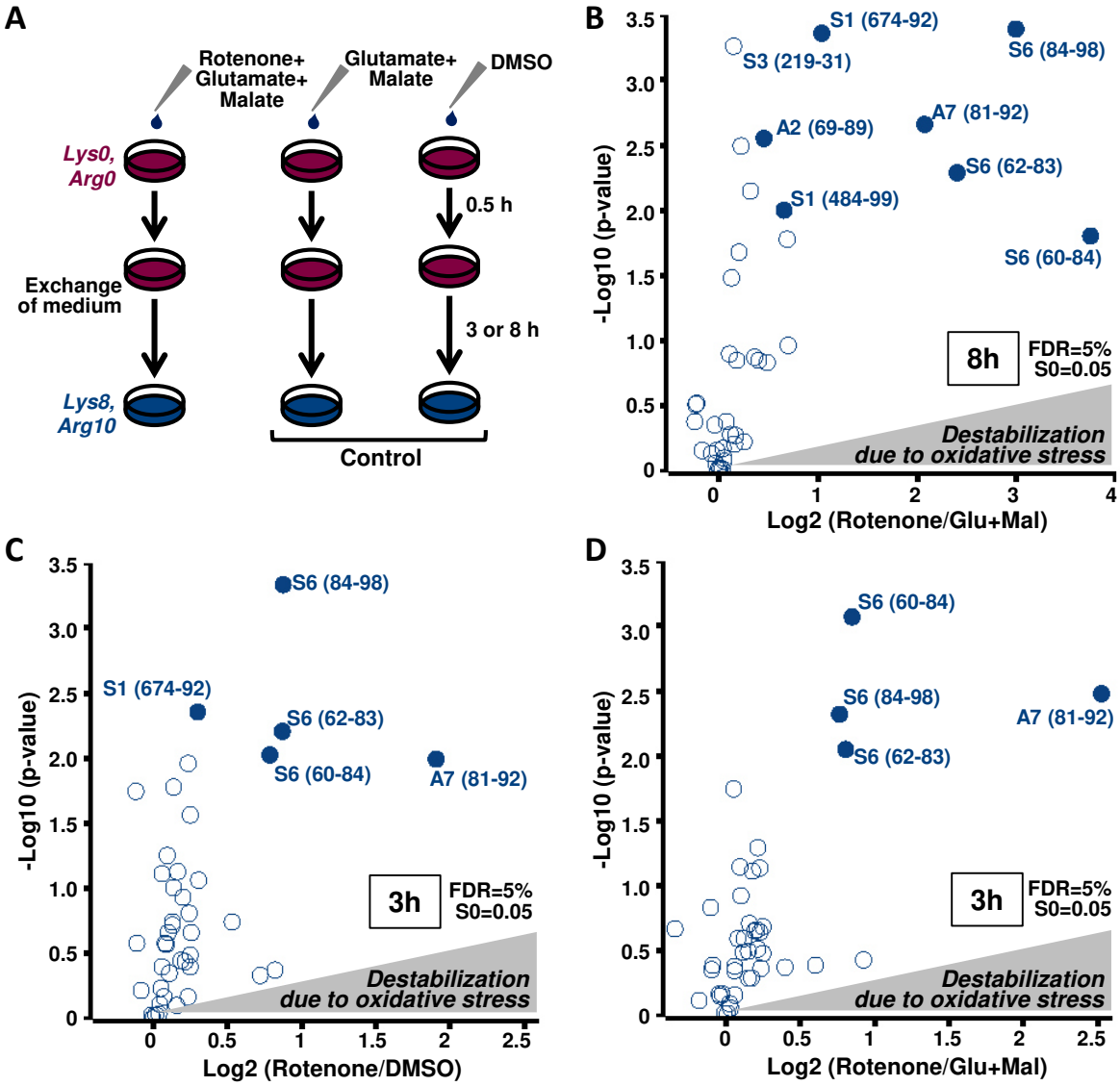
A
Rotenone+
Glutamate+
Malate
Glutamate+
Malate
DMSO
Lys0,
Arg0
0.5 h
Exchange
of medium
3 or 8 h
Lys8,
Arg10
Control
B
S1 (674-92)
S6 (84-98)
S3 (219-31)
A7 (81-92)
A2 (69-89)
S6 (62-83)
S1 (484-99)
S6 (60-84)
8h
FDR=5%
S0=0.05
Destabilization
due to oxidative stress
-Log10 (p-value)
Log2 (Rotenone/Glu+Mal)
C
S6 (84-98)
S1 (674-92)
S6 (62-83)
S6 (60-84)
A7 (81-92)
3h
FDR=5%
S0=0.05
Destabilization
due to oxidative stress
-Log10 (p-value)
Log2 (Rotenone/DMSO)
D
S6 (60-84)
S6 (84-98)
A7 (81-92)
S6 (62-83)
3h
FDR=5%
S0=0.05
Destabilization
due to oxidative stress
-Log10 (p-value)
Log2 (Rotenone/Glu+Mal)

Fig. S6

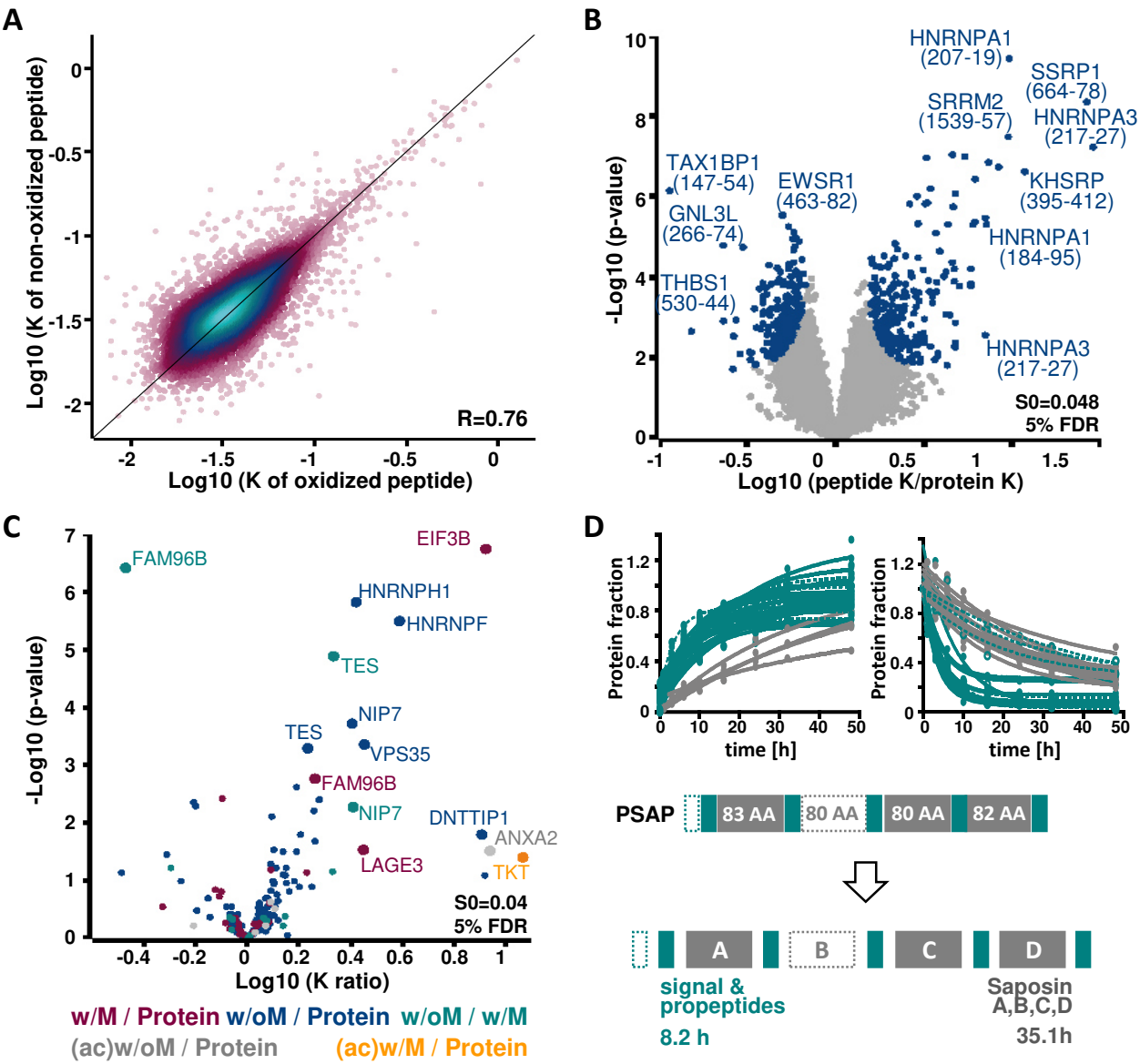
A
Log10 (K of non-oxidized peptide)
Log10 (K of oxidized peptide)
R=0.76
B
-Log10 (p-value)
Log10 (peptide K/protein K)
HNRNPA1 (207-19)
SSRP1 (664-78)
SRRM2 (1539-57)
HNRNPA3 (217-27)
TAX1BP1 (147-54)
EWSR1 (463-82)
KHSRP (395-412)
GNL3L (266-74)
HNRNPA1 (184-95)
THBS1 (530-44)
HNRNPA3 (217-27)
S0=0.048
5% FDR
C
-Log10 (p-value)
Log10 (K ratio)
EIF3B
FAM96B
HNRNPH1
HNRNPF
TES
NIP7
TES
VPS35
FAM96B
NIP7
DNTTIP1
ANXA2
LAGE3
TKT
S0=0.04
5% FDR
w/M / Protein
w/oM / Protein
w/oM / w/M
(ac)w/oM / Protein
(ac)w/M / Protein
D
Protein fraction
time [h]
PSAP
83 AA
80 AA
80 AA
82 AA
A
B
C
D
signal & propeptides
8.2 h
Saposin A,B,C,D
35.1h